An Acad Bras Cienc (2025) 97(2): e20240463 DOI 10.1590/0001-3765202520240463
Anais da Academia Brasileira de Ciências | *Annals of the Brazilian Academy of Sciences*
Printed ISSN 0001-3765 I Online ISSN 1678-2690
www.scielo.br/aabc | www.fb.com/aabcjournal

BIOMEDICAL SCIENCES

Chitosan/Maleic anhydride and Itaconic acid super porous hydrogels, containing levofloxacin for the treatment of visceral bleeding

SYEDA ALEENA UBAID, HAFIZ MUHAMMAD USMAN ABID, MUHAMMAD HANIF, KHALID MAHMOOD, MEMOONA QAYYUM & NABEELA AMEER

Abstract: Visceral bleeding poses a significant threat, requiring effective management through positively charged chitosan. This study aimed to address the limitations of chitosan-based hemostatic hydrogels by synthesizing a modified maleic anhydride complex of chitosan (MAC). Biocompatibility, biodegradability, and non-toxicity made MAC a suitable candidate for super porous hydrogels (SPHs) used in hemostatic applications. Graft polymerization synthesized MAC, confirmed via Fourier transform infrared spectroscopy, demonstrating superior antioxidant activity compared to chitosan and maleic anhydride. SPHs were prepared using MAC alone and with N, N-methylene bisacrylamide (MBA) as crosslinkers. MAC exhibited higher water absorbency and pH-dependent swelling than the MBA-chitosan complex. Drug loading and entrapment efficiency varied with the drug-to-SPH ratio. In vitro drug release studies showed sustained release (SR) with SPHs-MAC following zero-order kinetics and SPHs-MBA following Korsmeyer-Peppas. SPHs-MAC gelled more rapidly with temperature changes, and MAC hydrogels showed larger antimicrobial zones of inhibition (28±2).In vivo hemostasis studies revealed rapid hemostatic effects with MACL-H, reducing blood loss to 78.5 ± 1.5 mg in iver rat models. MAC hydrogels significantly lowered blood loss in rat tail amputation models compared to controls. This formulation demonstrates strong potential for effective visceral bleeding management.

Key words: Chitosan, maleic anhydride, super porous hydrogels, hemostasis, antimicrobial activity, in-vivo hemostasis

INTRODUCTION

Visceral bleeding, a life-threatening medical complication, requires effective management strategies which can occur as a result of trauma, gastrointestinal disorders, or other underlying medical conditions, poses a significant threat to patient well-being (Heneghan et al. 2012). Uncontrolled bleeding can lead to shock, organ damage, and even mortality if not promptly addressed (Pantalone et al. 2021). Over the years, various treatment options have been explored to address visceral bleeding. One such avenue involves the use of chitosan-containing polymers (Detsi et al. 2020). Chitosan has garnered attention due to its biocompatibility, biodegradability, and ability to promote hemostasis (Baharlouei & Rahman 2022). When incorporated into hydrogels, chitosan-based formulations have shown promise in controlling bleeding and supporting healing processes. Chitosan alone may not provide sufficient hemostatic efficacy in severe bleeding scenarios, necessitating the exploration of enhanced formulations (Saeedi et al. 2022). These variations may limit its applicability.

To overcome these limitations and enhance the utility of chitosan-containing polymers in

the management of visceral bleeding, it is imperative to explore innovative approaches and modifications. Chitosan can form complexes with metal ions like silver, copper, and iron, resulting in materials with antimicrobial properties (Messias et al. 2023). Depending on the metal used, there may be concerns about toxicity in certain applications. One promising solution to address the limitations of chitosan-based formulations involves the use of maleic anhydride (MA) as a crosslinker with chitosan.

Hydrogels composed of chitosan and alginate have been used for hemostasis (Ju et al. 2022). These hydrogels may not always achieve rapid hemostasis in cases of severe or high-pressure bleeding. They can also be prone to degradation in the presence of certain enzymes. Glycol chitosan can be combined with chitosan to create hydrogels for controlled drug delivery and hemostasis (Garshasbi et al. 2023). The viscosity of glycol chitosan can affect the ease of hydrogel application. These hydrogels may not be suitable for rapid hemostasis in large or deep wounds (Guo et al. 2022).

This approach will lead to the synthesis of a modified complex, denoted as MAC which will exhibits several advantageous properties, making it a suitable for the development of super porous hydrogels (SPHs) for hemostatic purposes. The synthesis of MAC will offer a promising solution to enhance chitosan-based hydrogels for hemostatic applications and will show favorable physicochemical properties, sustained drug release, and excellent hemostatic efficacy in in-vivo models, making it a potential candidate for managing visceral bleeding.

MATERIALS AND METHODS

Materials

Levofloxacin (molecular weight: 361.4 g/mol) was generously provided by Global Pharmaceuticals and served as the model drug. The polymer used was 95% deacetylated Chitosan (CT, molecular weight: 1526.5 g/mol). Maleic anhydride (MA, molecular weight: 98.06 g/mol), sodium hydroxide (NaOH, molecular weight: 39.997 g/mol), ammonium persulfate (APS, molecular weight: 228.18 g/mol) as the initiator, and methylene bisacrylamide (MBA, molecular weight: 154.17 g/mol) as the crosslinker were all procured from Sigma Aldrich Germany. Itaconic acid (molecular weight: 130.1 g/mol) was obtained from Merk Laboratory Germany, while acetic acid was sourced from Fisher Scientific Laboratory England. Acetone was purchased from BDH Laboratory. All chemicals, including double distilled water, were of analytical grade.

Synthesis of chitosan/Maleic anhydride cross-linker (MAC)

The synthesis of the chitosan maleic anhydride complex (MAC) was conducted through a one-step precipitation method. The dispersion phase began with the chitosan being continuously stirred for 30 minutes at room temperature in a 2% aqueous solution of acetic acid. In parallel, an aqueous solution known as the dispersed phase was created, which contained acetone and maleic anhydride in a 2.5:1 ratio. After 10 minutes in an ice bath, the dispersed phase was gradually added to the dispersion phase while being continuously stirred. After that, the suspension was left to stand at room temperature for a full day. The thickened mixture that had formed was gathered in 500 millilitres of acetone and then repeatedly cleaned with acetone three times before being submerged in water. Subsequently, it was vacuum-dried in a desiccator for 24 hours and stored in an airtight container for future use. The percentage yield was determined using the following formula:

$$\text{yield (\%)} = \frac{W2}{W1} \times 100 \quad (1)$$

W1 corresponds to the total weight of chitosan and maleic anhydride, whereas W2 represents the weight of the resultant MAC. The validation of interaction between unaltered polymers and the modified complex (MAC) was carried out utilizing Fourier transform infrared spectroscopy employing a Bruker Alpha instrument. Spectra were captured with 25 scans spanning the wavenumber range of 400-4000 cm^{-1}, and the mean value was presented to emphasize noticeable disparities in the -NH2 and -COOH peaks.

DPPH scavenging activity

Antioxidant activity of pure CT, MA and MAC was performed by already reported slightly modified method of Bakshi et al. (2020). Briefly, accurately measured 1ml aqueous solution of CT (2% acetic acid), MA (1% acetone) and MAC (1 % acetic acid) were added in 4 ml of ethanolic solution of DPPH (0.2 Mm). the resulted mixtures were allowed to stirred for 30 min at room temperature using different concentrations of CT, MA, MAC (10 to 100 µg/ml) and examining the antioxidant property by taking absorption at wavelength of 517nm Bakshi et al. (2020). The percentage antioxidant activity was calculated by using the following equation.

$$\text{Antioxidant activity (\%)} = \frac{A_c - A_s}{A\,C} \times 100 \quad (2)$$

where A_S is the sample's absorbance following DPPH reaction and A_C is the blank DPPH absorbance.

Preparation of super porous hydrogels

Two types of super porous hydrogels were made by slightly modified already reported free radical polymerization method. Briefly, equal amount of two types of crosslinker N, N-methylene bisacrylamide (N, N methylene-bisacrylamide) and freshly prepared modified MAC were compared for the preparation of two types of super porous hydrogels. In SPHs-I (MAC), aqueous solutions of chitosan (2% acetic acid) and itaconic acid were prepared, mixed with continuous stirring at room temperature until homogenized. Desired amount of aqueous solution of already described modified complex (MAC) was added into homogenous solution as crosslinker. APS was added for free radical polymerization. MBC was prepared according to above procedure by using the MBA as crosslinker in same ratio. All mixture solutions were degassed by passing nitrogen stream for 30 min and placed on water bath for copolymerization at 60 ^{O}C for first 2 h and continued at 70 ^{0}C for 24h. The resulted super porous hydrogels dried in oven at 45 ^{O}C, crushed and stored for further process (Suhail et al. 2023).

Physicochemical examination

Fourier transform infrared spectra was recorded on Bruker Alpha. Spectrum of both super porous hydrogels was recorded by placing small amounts of samples on diamond of Bruker Alpha I at wavenumber range 400-4000 cm^{-1} and average of 25 scans were reported and compared. X-ray diffraction (XRD) was performed for structural analysis of both SPHs.

To examine the water absorbing capacity, these super porous hydrogels were subjected to swelling measurement through tea bag method. Water retaining capacity was determined by placing the 100 mg of SPHs into a tea bag that was made of nylon cloth and completely immersed in distilled water at neutral pH and let soak at room temperature for 6h. The swollen gel was revealed the water absorbing capacity of the hydrogels, swollen gel was blotted with filter paper and change in weight was observed. The following equation was applied to calculate the water absorbency ratio and compared.

$$\text{water absorbency } \left(\frac{g}{g}\right) = Ws - \frac{Wd}{Wd} \quad (3)$$

where Ws and Wd stand for the two SPHs' respective swollen and dry weights. Dynamic and equilibrium swelling studies of two types of super porous hydrogels were performed by already described tea bag method. Weighed 10 mg of both SPHs (in tea bags) were soaked in three different pH (neutral, 1.2 and 7.4) aqueous buffer solutions at room temperature. After attaining the equilibrium swelling ratio (Q) at different time intervals both SPHs were taken out from buffer solutions, then blotted with filter paper to remove excess water from surface of samples and reweighed. Process was repeated for predetermined time intervals up to five days for dynamic swelling until constant weight for equilibrium swelling. The following formula was used to determine the swelling ratio.

$$\text{swelling ratio (Q)} = \frac{ws}{wo} \times 100 \quad (4)$$

Ws and wo shows swollen and dry weight of both SPHs respectively.

Drug loading and entrapment efficiency

150 mg of aqueous solution of drug levofloxacin was used for loading in both types of super porous hydrogels SPHs by soaking method. Both types of SPHs were soaked into 50ml of 5% aqueous solution of levofloxacin for 24h at room temperature. Drug loaded swollen and constant weight hydrogels were taken out from drug solution and removed residual drug and water from hydrogels surface by blotting with filter paper. Drug loaded SPHs were dried at room temperature first then in oven and completely dried, reweighed and stored for further use. Absorbance of 5% aqueous drug solutions was measured before and after the removal of SPHs from drug solution by using already constructed UV-vis calibrations curves of increasing concentration of levofloxacin at 292nm. For the confirmation of levofloxacin loading DLC % and entrapment efficiency EE % of hydrogels were calculated by the following equations.

$$\text{DLC (\%)} = \frac{wd}{wo} \times 100 \quad (5)$$

$$\text{EE (\%)} = dt - df/dt \times 100 \quad (6)$$

Whereas dt and df represent the amount of total drug and free drug, w_d and w_o represent the weight of drug loaded and unloaded SPHs.

In vitro drug release and kinetic studies

The percentage of drug released from both types of dried samples was investigated in room-temperature aqueous buffer solutions with pH values of 1.2 and 7.4. Levofloxacin loaded both SPHs were placed in 100ml of buffer solutions. After 1h 1ml of aliquot were withdrawn and replaced it by 1ml of fresh media. Process was repeated at predetermined time intervals and determined the %age drug released from withdrawn aliquot up to 12h by UV-visible spectroscopy and compared with calibration curve of levofloxacin at 292nm. All release study performed three times, mean of absorption values and compared with % age release of SPHs.

The in-vitro drug release characteristics from the polymeric matrix of two types of SPHs were examined utilizing various models including Higuchi model, Korsmeyer-Peppas model, time-dependent zero-order kinetics, concentration-dependent first-order kinetics, and Hixon-Crowell model. The drug release profile of SPHs incorporating MAC adhered to the zero-order model, while SPHs incorporating N, N MBA demonstrated behavior in line with the Korsmeyer-Peppas model, indicating a diffusion coefficient consistent with Non-fickian transport.

$$\text{Zero order kinetics: } F = F_0 + K_0 t \quad (7)$$

First order kinetics: $\ln F_1 = \ln F_o + K_o t$ 8)

Higuchi model: $Qt = k_H t^{0.5}$ (9)

Korsmeyer – peppas model: $Fk = \frac{Mt}{M} = Kptn$ (10)

Hixon Crowel: $Q_o - Q_t = -kc^{1/3}$ (11)

Here, the starting dose of the medication is represented by F_0 and Qo. Ft and Qt is the drug release fraction and the time constants for K0, K1, KH, Kp, and Kc. The drug's release amount at equilibrium and time (t) is expressed as Mt/M. n = exponent of drug release. Qo-Qt, the drug's initial and residual amounts at a given time (t). For drug release with zero order, n=1. For non-fickian drug release, n values between 1 and 0.45, and for fickian drug release, n ≤ 0.45.

Antimicrobial activity

The antimicrobial susceptibility assessment of MBC, MAC, MBCL-H, and MACL-H against multidrug-resistant *E. coli* and *S. aureus* was conducted following a modified version of the method. In short, 20 millilitres of sterilized Mueller-Hinton Agar were heated to 120°C, then aseptically transferred into petri plates that had been sterilized. It was then allowed to solidify at 37°C. After dilution in nutrient broth to reach an optical density of 0.5, bacterial cultures were incubated at 37°C for a full day. Muller Hinton (MH) agar plates were prepared. Using a sterile cotton swab, evenly spread 100µl of bacterial suspension (1×10^5 CFU/ml) onto the plates. Aseptically, 3 mm-diameter wells were made on each MH agar plate. The plates were then incubated at 37°C for 24 hours after 4 mg/ml (100µl) of MBC, MAC, MBCL-H, and MACL-H were directly added to the wells. Each sample's zone of inhibition was measured following incubation. To guarantee that the results could be trusted, each experiment was carried out three times.

In-vivo hemostasis activities

Rat liver hemostasis

Rats were anesthetized, and their abdomens were shaved and disinfected with 75% alcohol. Following careful incision of the abdominal cavity, a liver section was extracted to create a wound approximately 0.5 cm in length, resulting in spontaneous bleeding for 5 seconds. The bleeding site was then gently wiped with gauze, and the test sample was applied to the wound. The bleeding condition was monitored, and the time taken for bleeding cessation was recorded. The hemostatic dressing was subsequently weighed to determine the amount of blood absorbed, and the average value from six parallel experiments was considered for analysis.

Hemostasis of rat tail amputation

The hemostatic effectiveness was evaluated using a rat tail amputation model following the established procedure outlined by Xiang et al. (2022) seven rats were employed for this assessment. The rats were given chloroform anesthesia, and after having their tails cut with surgical blades 1 cm from the tip, their blood was collected on medical gauze. The Mettler Toledo Precision Balance was used to weigh the gauze both before and after the incision. The duration required for bleeding to stop from the tail was noted as the baseline control. For the remaining three rats, their tails were similarly amputated 1 cm, and then 5 mg of chitosan, MBCL-H, and MACL-H, respectively, were applied to the incision site. The time until bleeding cessation was recorded. The average of six experiments was calculated and reported with their mean ± standard deviation (n = 6)(Xiang et al. 2022).

SEM analysis

SEM (Hitachi High Tech S4900 FE-SEM) was implied to evaluate the morphology of MBCL-H

and MACL-H hydrogel samples. MBCL-H and MACL-H was added on a sample holder with a 20 kV at 1,5 and 10µm to in a dry condition.

RESULTS AND DISCUSSION

MAC and super porous hydrogels SPHs

Modified MAC was prepared as a crosslinker by graft polymerization and precipitation method. Here grafted the maleic anhydride (MA) onto chitosan which introduced its carboxyl group with NH_2 group of chitosan, the mechanism involved in the synthesis of MAC and further reaction process for the synthesis of super porous hydrogels is shown in chemical scheme Figure 1. In this study the two types of super porous hydrogels were prepared by using two types of crosslinkers N, N methylene-bisacrylamide (N, N MBA) and already described modified complex (MAC). The MACL-H was prepared by mixing the aqueous solutions of modified MAC with chitosan and itaconic acid interpolymeric complex (CS/IA) solutions with continuous stirring by adding APS initiator for free radical polymerization to homogenize the solutions. The MBCL-H was prepared by above

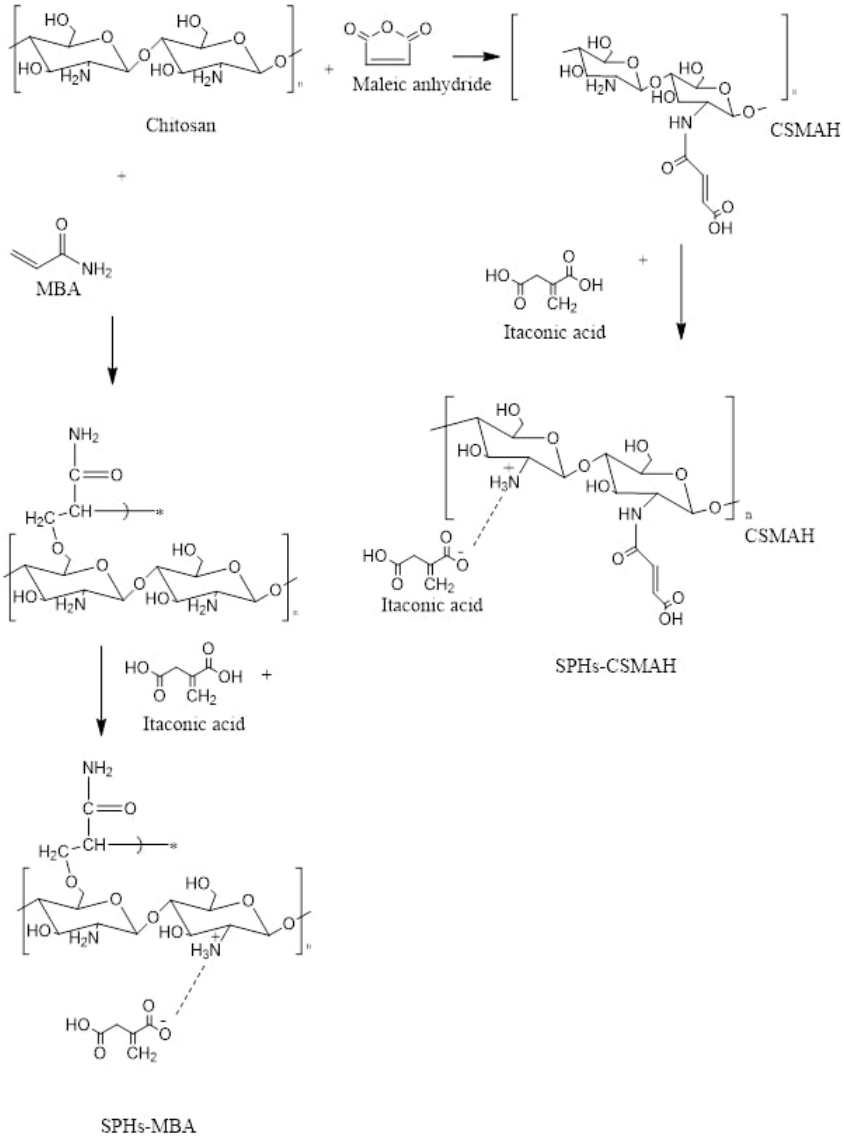

Figure 1. Chemical scheme of MBA and CSMAH super porous hydrogels.

describe procedure by using aqueous solution of methylenebisacrylamide (MBA) as a crosslinker, here vinyl group of MBAs bind to the OH group of C6 chitosan polymers for crosslinking. Both homogenous solutions were passed through nitrogen stream for 30 min to remove the oxygen content in solutions. Heating is required for the copolymerization therefore both solutions were placed into water bath for copolymerization. At 40-60 ^{0}C there was no crosslinking occurs then increase the temperature up to 70 ^{0}C then complete polymerization occurred within 24h to formed the gels and the resulted gels were dried and crushed to synthesized the two super porous hydrogels. crosslinkers were compared by performing the swelling studies, absorbing capacity, % age drug loading and %age entrapment efficiencies, FTIR, SEM and XRD.

DPPH scavenging activity

Pure CT, MA, and MAC's antioxidant potential was confirmed by their ability to scavenge free radicals in DPPH, as shown by their colour changing from purple to yellow. When the concentrations of CT, MA, and MAC were varied, the antioxidant capacity of DPPH was evaluated, and the results showed that the compounds' antioxidant properties increased from 10 mg/ml to 100 µg/ml. MAC demonstrated the highest DPPH free radical scavenging activity at 80 µg/mL, with a value of 70 ± 2%, in contrast to CT (63 ± 2%) and MA (44 ± 2%). A summary of the antioxidant activity results is shown in Figure 2, which also shows the percentage of concentration-based scavenging activity.

Physicochemical examination, water absorbency measurement, dynamic and equilibrium swelling of super porous hydrogels

Using Fourier-transform infrared spectroscopy (FTIR), the study synthesised a modified complex called MAC and investigated crosslinking interactions between polymers, monomers, and crosslinking agents. The spectra of itaconic

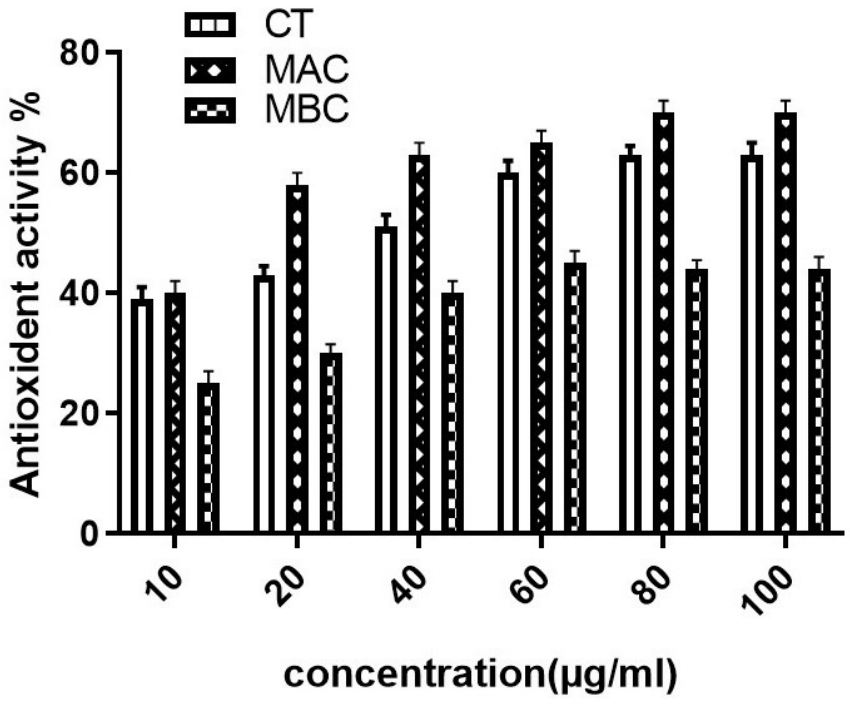

Figure 2. Comparison of antioxidant properties of CT (Chitosan), MAC (Maleic anhydride Chitosan complex) and MBC (Methylene bisacrylamide Chitosan complex) at different concentrations.

acid, maleic anhydride (MAH), grafted chitosan by maleic anhydride (MAC), pure chitosan (CS), both crosslinkers (MAC & N, N MBA), and both SPHs are shown in Figure 4. A notable peak of pure chitosan was found at 3309 cm-1, which indicated stretching of the hydroxyl and amide group (OH-NH2). Other notable peaks were found at 2800-3000 cm-1, attributed to (C-H) stretching, at 1550 cm-1, indicated amide I and II bending, and at 1077 cm-1, was attributed to (C-O stretching). Peaks in the range of 890–1060 cm-1 were ascribed to pyranose ring chain stretching, whereas peaks in the range of 1380–1450 cm-1 were noted as a result of CH3 group deformation. New peaks appeared in the MAC spectrum between 1650 and 1589 cm-1, indicating that the maleic anhydride C-O group ring has opened. In the MAC spectrum, the amide band-corresponding peaks disappeared. Furthermore, a new peak arose at 1773 cm-1 as a result of maleic anhydride's C=O vibration stretching, and new peaks arose in the 1354 cm-1 to 1461 cm-1 range as a result of the overlapping of C-H bending and C-N stretching. Along with peaks at 3700 cm-1 related to OH stretching, Figure 4a showed a broad peak at 1440 cm-1 and 1564 cm-1, which confirmed the formation of an interpolymeric complex from NH3+ and COO- interactions. Furthermore, moderate peaks were seen at 2990 cm-1 and 3150 cm-1, indicating the interaction of MBA's C=O-NH2 with chitosan, while new peaks arose at 1770 cm-1 as a result of carbonyl stretching. Additionally, Figure 4's FTIR spectra showed how all of the functional groups interacted with one another, supporting the formation of both SPHs.

Both SPHs were weighed into a tea bag containing approximately 150 mg of water, and the tea bag was then submerged in distilled water for six hours at room temperature in order to measure the water-absorbing capacity. Both samples were removed after six hours, weighed again, and their water-retaining capacity was calculated as the percentage of the difference in weight between the two dry SPHs. The water-absorbing capacity of SPHs-CSMAH was 82%, whereas SPHs-MBA had a capacity of 62%. The modified complex CSMAH-containing SPHs were found to have a greater capacity for water absorption.

Three distinct aqueous buffer solutions with pH values of 1.2, neutral, and 7.3 were used to study the swelling of both SPHs based on pH at room temperature. In order to achieve this, the two dried SPH samples were soaked in aqueous buffer solutions with pH values of 1.2, neutral, and 7.4, and the rate of change in weight over various time intervals was recorded. In this investigation, the low swelling rate (Q) was demonstrated at low pH 1.2 and increased swelling rate (Q) at high pH 7.4. Figure 5 illustrates the slight swelling of both SPHs in neutral pH aqueous solution. Due to the presence of polymers that remain ionized as chitosan is protonated in highly acidic solutions and the formation of strong hydrogen bonds, which prevent water from diffusing into the porous network of SPHs and reduce the swelling index, the swelling rate decreased at a highly acidic pH of 1.2 (Malik et al. 2020). Due to the unionized polymers' non-protonated carboxyl group and the absence of hydrogen bonding, which increased the repulsive forces within itaconic chains and allowed the solutions to diffuse into polymeric networks and raise the swelling index of SPHs, the swelling rate was extremely high at high alkaline pH 7.4 (Tan et al. 2022). Both SPHs showed swelling behavior at neutral pH, the reason behind this highly porous network of SPHs permits the uplifting of water and increased the water absorbing capacity. In comparative study exhibited the effect of crosslinker on the swelling rate (Q), that the SPHs-MBA using the N, N MBA which increase the crosslinking

density by engaging the OH group of chitosan which formed the more compact network and decreased the diffusion of water into hydrogels network than the SPHs-CSMAH. However, by increasing in crosslinking density the swelling rate was decreased (Rohm et al. 2019).

Drug loading and entrapment efficiency

Drug entrapment efficiency was stated as percentage of drug entrapped within in the polymeric network from total drug loaded content of both super porous hydrogels measured by using equation (5). The percentage of drug entrapment efficiency was calculated by taking different ratios of drug and polymeric SPHs that changes from 80% to 69% in SPHs-CSMAH and from 65% to 57% in SPHs-MBA. The percentage of drug entrapment efficiency was calculated by varying the drug and both polymeric SPHs ratios such as 1:1, 1:2 and 1:3 and examined the variations in entrapment efficiency. The obtained result showed that by increasing the drug and polymeric SPHs ratio will cause an increase in entrapment efficiency but further increase caused the decrease of entrapment efficiency. In Supplementary Figure - S1, increase in drug: SPHs (1:1 to 1:2) tends to increased form 78% to 81% in SPHs-CSMAH and 63% to 67% in SPHs-MBA, because more polymeric contents of SPHs cause more interaction to solvents and entrapped the drug within porous network but further increased in ratio (1:2 to 1:3) cause decreased in entrapment efficiency within range of 81% to 69% in SPHs-MAC and from 67% to 57% in SPHs-MBA, the increased in ratios was significantly increases the polymeric concentrations that caused the increase in viscosity and crosslinking density which hinders to entanglement of drug solution within porous network. So, concluded that by increasing the drug and SPHs ratio showed positive result but further increase expressed its negative result on drug entrapment efficiency of both SPHs (Mahmood et al. 2023).

In vitro drug release and kinetic studies

As illustrated in Figure S1, the percentage drug release from the two levofloxacin-loaded SPHs was examined using the dialysis bag diffusion method in buffer aqueous solution at pH 1.2 & 7.4 for 12 hours. The percentage of drug release curves for both SPHs showed that the drug released more when the pH increased. For example, the drug released more slowly in the first three hours, just like in cases of swelling, and the percentage of drug release increased at higher alkaline pH 7.4. The amount of drug loaded within the porous network of SPHs and the swelling behavior determine the percentage of drug release. The outcome of the experiment demonstrated that as pH increased, so did the percentage of drug released, and this was followed by an increase in SPH swelling. Because of their more porous nature, which causes more swelling and faster drug release than SPHs-MBA, it was found that SPHs-MAC, which have higher porosity and lower crosslinking density at higher pH, provide more surface area and exhibit a greater percentage of drug release.

Super porous hydrogels (SPHs) showed a gradual release of drugs while retaining their porous integrity and flexibility, according to in vitro drug release studies. Interestingly, it was discovered that the drug released more quickly at higher pH values than it did at lower pH levels (1.2). The drug release kinetics were examined using a variety of mathematical modelling techniques, such as zero order, first order, Korsmeyer-Peppas, Higuchi, and Hixon-Crowell models. SPHs-MAC adhered to the zero-order model, while SPHs-MBA followed the Korsmeyer-Peppas model, according to an analysis of the drug release data. The values of the release coefficient (N) and regression coefficient (R2)

that were obtained for the SPHs-MAC and SPHs-MBA, respectively, were 0.345 and 0.264, indicating a non-Fickian transport mechanism for the sustained release of levofloxacin.

Effect of temperature in onset of gelation

The effect of temperature on the time required for the gelling of polymers and monomers in the presence of comparative crosslinking agents to form porous and flexible SPHs was studied. while in free radical polymerization method, temperature must be required in crosslinking the polymers for the onset of gelation. As an increase in temperature caused increase in the crosslinking of polymers and monomers which decreased the time for onset of gelation as shown in Figure S2. Comparative study displayed that SPHs-MAC with anhydride components increases the crosslinking of polymers and monomers which cause the rapid gelation as compared to SPHs-MBA showing more onset of gelation time for the formation of stable flexible and highly porous hydrogels.

Antimicrobial activity

Minimum and maximum Zone of inhibition (ZOI) of the MBC, MAC, MBCL-H and MACL-H was shown in Figure 3. In case of G -ve bacteria i.e., *E. coli*, maximum zone of inhibition of MBC, MAC, MBCL-H and MACL-H were 18 ±2, 23 ±2, 24 ±2, 32 ±2 respectively. While in case of G +ve bacteria i.e., *S. aureus* maximum zone of inhibition of MBC, MAC, MBCL-H and MACL-H were 19±2, 21±2, 22±2, 28±2 respectively. Increased in ZOI against *E. coli* may be due to the presence of pores in outer membrane of G -ve bacteria. G +ve bacteria i.e., *S. aureus* lack outer membrane which makes G -ve bacteria more susceptible towards formulations than G +ve ones.

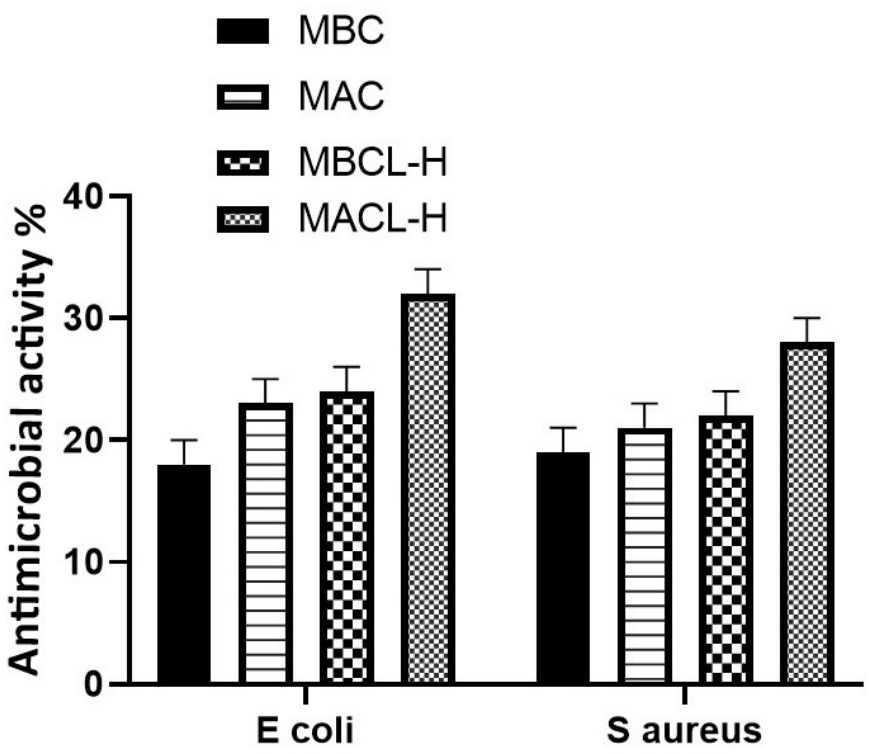

Figure 3. Antimicrobial activity of MBC, MAC, MBCL-H and MACL-H at different concentrations.

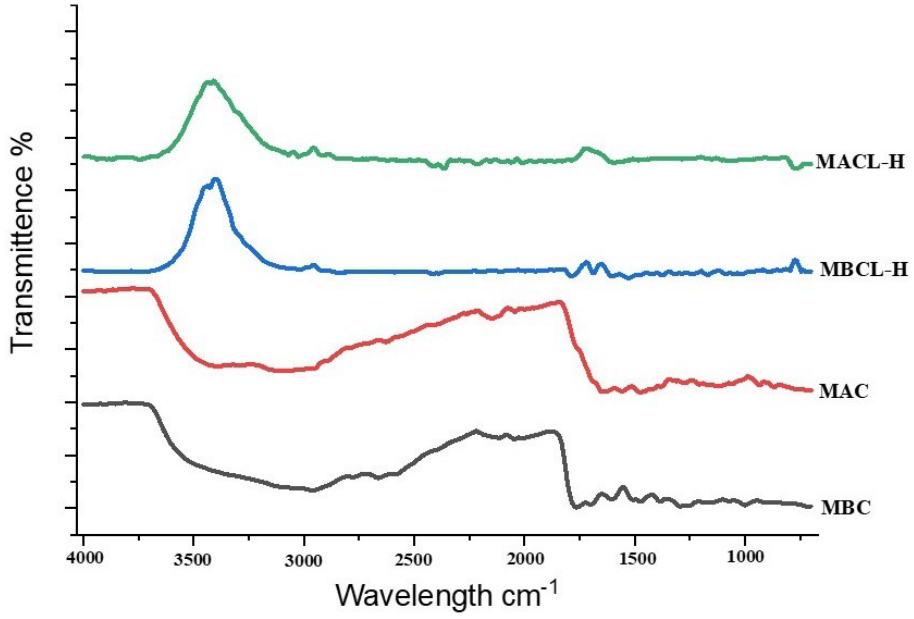

Figure 4. FTIR analysis of MACL-H, MBCL-H, MAC and MBC.

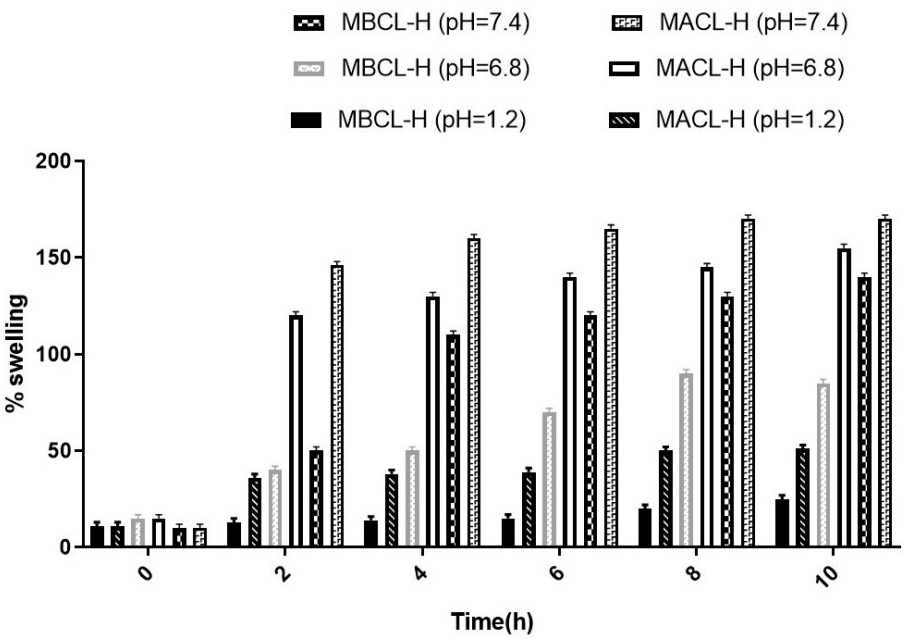

Figure 5. Age swelling % of super porous hydrogels at three different pH, at pH=1.2 (A), pH=6.8 (B), pH=7.4 (C).

In-vivo hemostasis activities

Rat liver hemostasis

Figure S3a illustrates the hemostasis time in rat liver. In the blank control group without treatment, bleeding persisted after 3.5 minutes, whereas hemostasis was achieved within 1 minute in the CT, MACL-H, and MBCL-H groups, indicating a highly significant difference compared to the blank control groups ($p < 0.01$). Compared to the control, the hemostatic time of MACL-H was 55 ± 1 second ($n = 6$), which was statistically significant ($p < 0.05$). Even without applying pressure, MACL-H effectively controlled liver bleeding within 60 seconds. In contrast, bleeding persisted significantly beyond 120

seconds in the Control, CT, and MBCL-H groups. After the hydrogel treatment, the blood loss in the liver was significantly reduced to 78.5 ± 1.5 mg, while it was 305.6 ± 15 mg, 209 ± 10 mg, and 160 ± 12 mg in the Control, CT, and MBCL-H groups, respectively. Furthermore, the blood clot area on the filter paper provided additional evidence of the hydrogel's hemostatic action. Quick adherence of the ultra-porous hydrogel to the injured tissues allowed for quick hemostasis. In conclusion, the MACL-H hydrogel exhibited an excellent liver hemostatic effect, significantly reducing organ bleeding. The study evaluates the effectiveness of different formulations, including chitosan (CT), Maleic anhydride-chitosan-levofloxacin superporous hydrogels (MACL-H), and methylene bisacrylamide-chitosan-levofloxacin superporous hydrogels (MBCL-H), in achieving hemostasis. The untreated blank control group serves as a baseline for comparison.

The effectiveness of chitosan-based hydrogels, exemplified by MACL-H and MBCL-H, aligns with existing literature. Chitosan, a biocompatible and biodegradable polysaccharide, is well-studied for its hemostatic properties. Its gel-forming ability and promotion of platelet adhesion make it a promising candidate for hemostatic applications (Bakshi et al. 2020). The incorporation of levofloxacin further enhances functionality, potentially addressing concurrent infections in traumatic injuries.

The utilization of superporous hydrogels, demonstrated by the MACL-H, introduces a novel approach to hemostasis. The porous structure likely facilitates rapid blood absorption and clotting, contributing to the observed accelerated hemostasis. The inclusion of maleic anhydride in the hydrogel formulations may impart additional properties, such as improved mechanical strength and enhanced tissue adhesion.

Hemostasis of rat tail amputation

Rats were used in tail cutting experiments to learn more about the hemostatic effectiveness of the control, CT, MACL-H, and MBCL-H groups on diffuse bleeding in Figure S3b. The results showed that within 90 seconds, caudal vein hemorrhage was successfully controlled by CT, MBCL-H, and MACL-H, with total blood losses of 290 ± 2.1 mg, 210 ± 1.5 mg, and 180.3 ± 1.6 mg, respectively. On the other hand, the control group experienced considerable bleeding that continued for more than three minutes, leading to a total blood loss of 740 ± 30 mg. In comparison to the blank control group, the hemostasis times of the CT, MACL-H, and MBCL-H groups were significantly shorter ($p < 0.01$).

SEM analysis

The SEM images (Figure S4) reveal significant porosity of MACL-H and MBCL-H hydrogels. MACL-H (a, a1, a2) shows a uniform, highly porous structure with interconnected pores, indicative of optimal porosity for enhanced fluid absorption and drug delivery

CONCLUSIONS

The MAC synthesis offers a promising solution to enhance chitosan-based hydrogels for hemostatic applications. MACL-H showed favorable physicochemical properties, sustained drug release, and excellent hemostatic efficacy in in-vivo models, making it a potential candidate for managing visceral bleeding.

Acknowledgments

The authors extend their gratitude to the Department of Pharmaceutics, Faculty of Pharmacy, Bahauddin Zakariya University Multan, for generously granting access to research facilities. Additionally, the Higher

Education Commission (HEC) of Pakistan deserves acknowledgment for approving the study.

SUPPLEMENTARY MATERIAL

Figures S1-S4.

REFERENCES

BAHARLOUEI P & RAHMAN A. 2022. Chitin and chitosan: Prospective biomedical applications in drug delivery, cancer treatment, and wound healing. Marine Drugs 20: 460.

BAKSHI PS, SELVAKUMAR D, KADIRVELU K & KUMAR N. 2020. Chitosan as an environment friendly biomaterial–a review on recent modifications and applications. Int J Biol Macromol 150: 1072-1083.

DETSI A, KAVETSOU E, KOSTOPOULOU I, PITTEROU I, PONTILLO ARN, TZANI A, CHRISTODOULOU P, SILIACHLI A & ZOUMPOULAKIS P. 2020. Nanosystems for the encapsulation of natural products: The case of chitosan biopolymer as a matrix. Pharmaceutics 12: 669.

GARSHASBI H, SALEHI S, NAGHIB SM, GHORBANZADEH S & ZHANG W. 2023. Stimuli-responsive injectable chitosan-based hydrogels for controlled drug delivery systems. Front Bioeng Biotechnol 10: 1126774.

GUO H, HUANG S, XU A & XUE W. 2022. Injectable adhesive self-healing multiple-dynamic-bond crosslinked hydrogel with photothermal antibacterial activity for infected wound healing. Chem Mater 34: 2655-2671.

HENEGHAN HM, MERON-ELDAR S, YENUMULA P, ROGULA T, BRETHAUER SA & SCHAUER PR. 2012. Incidence and management of bleeding complications after gastric bypass surgery in the morbidly obese. Surgery for Obesity and Related Diseases 8: 729-735.

JU J, KIM J, CHOI Y, JIN S, KIM S, SON D & SHIN M. 2022. Punicalagin-loaded alginate/chitosan-gallol hydrogels for efficient wound repair and hemostasis. Polymers 14: 3248.

MAHMOOD A, ERUM A, TULAIN UR, SHAFIQ S, MALIK NS, SIDRA, KHAN MT & ALQAHTANI MS. 2023. Aloe vera-Based Polymeric Network: A Promising Approach for Sustained Drug Delivery, Development, Characterization, and In Vitro Evaluation. Gels 9: 474.

MALIK NS, AHMAD M, MINHAS MU, TULAIN R, BARKAT K, KHALID I & KHALID Q. 2020. Chitosan/xanthan gum based hydrogels as potential carrier for an antiviral drug: Fabrication, characterization, and safety evaluation. Front Chem 8: 50.

MESSIAS I, DE FREITAS MARIN CF, LAZARIN-BIDÓIA D, NAKAMURA CV, RUBIRA AF, SILVA R & FOLLMANN HDM. 2023. Enhanced Bactericidal Effect of Chitosan Using Coordinated Transition Metal Ions. J Inorg Organomet Polym Mater 34: 511-521.

PANTALONE D, BERGAMINI C, MARTELLUCCI J, ALEMANNO G, BRUSCINO A, MALTINTI G, SHEITERLE M, VILIGIARDI R, PANCONESI R & GUAGNI T. 2021. The role of damps in burns and hemorrhagic shock immune response: pathophysiology and clinical issues. Review. Int J Mol Sci 22: 7020.

ROHM K, MANAS-ZLOCZOWER I & FEKE D. 2019. Poly (HIPE) morphology, crosslink density, and mechanical properties influenced by surfactant concentration and composition. Colloids and Surfaces A: Physicochemical and Engineering Aspects 583: 123913.

SAEEDI M, VAHIDI O, MOGHBELI MR, AHMADI S, ASADNIA M, AKHAVAN O, SEIDI F, RABIEE M, SAEB MR & WEBSTER TJ. 2022. Customizing nano-chitosan for sustainable drug delivery. Journal of Controlled Release 350: 175-192.

SUHAIL M, CHIU I-H, LAI Y-R, KHAN A, AL-SOWAYAN NS, ULLAH H & WU P-C. 2023. Xanthan-Gum/Pluronic-F-127-Based-Drug-Loaded Polymeric Hydrogels Synthesized by Free Radical Polymerization Technique for Management of Attention-Deficit/Hyperactivity Disorder. Gels 9: 640.

TAN RYH, LEE CS, PICHIKA MR, CHENG SF & LAM KY. 2022. PH responsive polyurethane for the advancement of biomedical and drug delivery. Polymers 14: 1672.

XIANG J, WANG Y, YANG L, ZHANG X, HONG Y & SHEN L. 2022. A novel hydrogel based on Bletilla striata polysaccharide for rapid hemostasis: Synthesis, characterization and evaluation. Int J Biol Macromol 196: 1-12.

How to cite

UBAID SA, ABID HMU, HANIF M, MAHMOOD K, QAYYUM M & AMEER N. 2025. Chitosan/Maleic anhydride and Itaconic acid super porous hydrogels, containing levofloxacin for the treatment of visceral bleeding. An Acad Bras Cienc 97: e20240463. DOI 10.1590/0001-3765202520240463.

Manuscript received on May 17, 2024;
accepted for publication on January 23, 2025

SYEDA ALEENA UBAID[1]
http://orcid.org/0009-0002-0878-288X

HAFIZ MUHAMMAD USMAN ABID[1]
http://orcid.org/0000-0001-8881-9181

MUHAMMAD HANIF[1]
http://orcid.org/0000-0002-2303-3804

KHALID MAHMOOD[1,2]
http://orcid.org/0000-0003-1025-5800

MEMOONA QAYYUM[1]
https://orcid.org/0009-0001-2939-941X

NABEELA AMEER[1]
https://orcid.org/0009-0006-2923-489X

[1]Bahauddin Zakariya University Multan, Department of Pharmaceutics, Faculty of Pharmacy, 60800 Multan, Pakistan

[2]Bahauddin Zakariya University Multan, Institute of Chemical Sciences, 60800 Multan, Pakistan

Correspondence to: **Muhammad Hanif, Khalid Mahmood**
E-mail: muhammad.hanif@bzu.edu.pk, kmchemist@yahoo.com

Author contributions

Syeda Aleena Ubaid: Conceptualization, Data curation, Methodology, Project administration, writing original draft. Hafiz Muhammad Usman Abid: Conceptualization, Project administration. Muhammad Hanif: Conceptualization, supervision, Investigation, Project administration, resources. Khalid Mahmood: Formal analysis. Memoona Qayyum: Software, visualization. Nabeela Ameer: Validation.